

A BRIGHT OPTICAL SYNCHROTRON COUNTERPART OF THE WESTERN HOT SPOT IN PICTOR A^{1,2}

HERMANN-JOSEF RÖSER

Max-Planck-Institut für Astronomie

AND

KLAUS MEISENHEIMER

Royal Observatory, Edinburgh

Received 1986 May 20; accepted 1986 August 19

ABSTRACT

A $B = 19.5$ mag bright, highly polarized ($P > 30\%$) object was detected close to the western hot spot in Pictor A during an optical polarization survey of radio hot spots in classical double radio sources. The unresolved source exhibits a featureless continuum between 400 and 800 nm and is identified as the optical counterpart of the radio hot spot. It is surrounded by optical filaments aligned roughly perpendicular to the source axis. The hot spot is also marginally detected in an *Einstein* IPC frame.

Subject headings: galaxies: individual — galaxies: structure — polarization — radiation mechanisms — radio sources: galaxies

I. INTRODUCTION

Studies of optical synchrotron radiation from radio hot spots allow us to determine their overall spectrum over a broad frequency range and thus provide important constraints on the particle acceleration mechanism in radio lobes (Laing 1984; Meisenheimer and Heavens 1986). In particular, optical synchrotron radiation more closely maps the sites of particle acceleration than radio observations do because of the short lifetimes of the radiating particles.

Although faint optical objects have been found at or near several hot spot locations (Crane, Tyson, and Saslaw 1983) their nature is unclear. They may well be unrelated foreground objects. For 3C 33 (south), however, we could show, through a perfect match between optical and radio polarization data, that the optical radiation is also of synchrotron origin (Meisenheimer and Röser 1986, hereafter MR). Furthermore, it exhibits a synchrotron cutoff spectrum similar to the one found in 3C 273A (Röser and Meisenheimer 1986, hereafter RM).

We have, therefore, begun an optical polarization survey of radio hot spots. Sources were selected mainly from a well-defined sample of 166 3CR sources, for which five GHz Cambridge maps are available in the literature (Jenkins, Pooley, and Riley 1977). In addition, several bright southern sources were also included.

Here we report our first results for the western hot spot of the double lobe source Pictor A (0518–456), which was selected for observations because of its brightness (67 Jy at 408 MHz) and pronounced linear polarization on low-resolution radio maps (Schwarz, Whiteoak, and Cole 1974; Schilizzi and McAdam 1975; Christiansen *et al.* 1977). It was only after our observations had been performed that we realized the availability of a VLA map with moderate resolution (Prestage 1985).

II. OBSERVATIONS AND DATA ANALYSIS

The low resolution of the available radio maps and the fact that the peak in optical brightness does not necessarily coincide with the radio maximum (RM) demand two-dimensional imaging polarimetry of all objects in the radio hot spot vicinity to search for polarized objects. Ordinary and extraordinary images of all objects were recorded simultaneously by placing a double calcite (Savart) plate in front of the focal plane (Röser 1981).

Observations of Pictor A (west) were carried out at the ESO 3.6 m telescope on La Silla with the ESO Faint Object Spectrograph and Camera (EFOSC) (Buzzoni *et al.* 1984) on 1985 November 8 and 9. In the first night the Savart plate was mounted in the diverging beam behind the aperture wheel. The image separation of 1500 μm corresponded to $10''$ on the sky. The field of view was $\sim 2.5 \times 2.5$ square. Two exposures of the field of Pictor A (west) were obtained through a B-filter in this configuration: a short (1 minute) acquisition frame and a long (20 minutes) science frame, both with the same orientation of the instrument rotator (north-south image separation caused by the Savart plate). Seeing was $\sim 2''.5$.

The Savart plate had to be removed for the second night to enable spectroscopy and direct imaging. Spectra of 50 and 60 minutes total exposure time, respectively, were obtained at 0.8 nm pixel⁻¹ with a red- and a blue-blazed grating. Finally deep direct exposures of 15 minutes (twice) and 10 minutes (once) were taken in the blue and in a red filter, respectively. Seeing was $1''.5$.

All exposures were corrected for DC offset and flat field. The flat fields for spectroscopic frames were obtained from a continuum lamp exposure, for imaging observations from object frames as described by MR.

III. RESULTS

a) Polarimetry

On the science exposure of Pictor A (west) taken through the Savart plate, a highly polarized object stands out (Fig. 1). From the magnitude difference between ordinary and extraordinary

¹ Based on observations collected at the European Southern Observatory, La Silla, Chile.

² H. J. R. would like to dedicate this work to Prof. R. Kippenhahn on the occasion of his 60th birthday.

image a lower limit to the linear polarization of $29.6\% \pm 0.8\%$ is derived. Because of the lack of further frames with other orientations of the Savart plate, only this limit, and no polarization angle, can be deduced. Analysis of the acquisition frame qualitatively yielded the same.

b) Direct Imaging (Astrometry and Photometry)

The polarized source is visible on the ESO Quick Blue Sky Survey as a stellar object of ~ 19 mag. Its position as measured from a glass copy of the sky survey plate is

$$\alpha(1950) = 5 \text{ h } 18 \text{ min } 0.09 \text{ s} \pm 0.08 \text{ s},$$

$$\delta(1950) = -45^\circ 48' 53''.9 \pm 0''.7.$$

This is within $3''$ of the radio position quoted by Prestage (1985) on the basis of VLA data taken with a beam of $\sim 10'' \times 25''$ (see Fig. 2). We therefore identify the highly polarized source with the radio hot spot. Note that earlier radio positions (e.g., Schilizzi and McAdam 1975) differ by more than $1'$ from the VLA position.

The deep direct exposures show structures surrounding the hot spot location (Fig. 2). A secondary brightness maximum is located $\sim 4''$ toward the central source. Two parallel filaments of $15''$ length cut through the immediate hot spot area at about right angles to the axis central source hot spot.

Fluxes of the bright component were derived from the direct images using measurements of only a few standard stars. No color terms were determined, since the night was not photometric. Nevertheless our values of $f_\nu(4.27 \times 10^{14} \text{ Hz}) = 130$

MJy and $f_\nu(6.98 \times 10^{14} \text{ Hz}) = 68 \text{ MJy}$ are consistent with the flux as derived independently from the spectra. We are thus confident that the errors are not too large, on the order of 20% or less.

c) Spectroscopy

The sky-subtracted, superposed data from two blue and two red spectra are shown in Figures 3a and 3b, respectively. Because of various problems encountered in the consistent removal of the instrumental response over the whole frequency range from two standard star measurements in each bandpass, we only show the normalized data. Neither emission nor absorption features of significance can be found with an equivalent width greater than 0.3 nm for a width of smaller than 2 nm (i.e., the formal values derived for the "feature" seen at 443 nm in the blue spectrum).

d) X-Ray Data

IPC data taken by the *Einstein Observatory* in a 1700 s exposure were kindly supplied from the *Einstein* data bank (Fig. 4). An extension from the central source is evident at P.A. 280° , which we tentatively identify with the hot spot. From a comparison with two other faint sources in the field we estimate the X-ray flux to be somewhat less than 90 nJy at $5 \times 10^{17} \text{ Hz}$. Statistical significance of the counterpart is only marginal, however, as was shown by Seward and Aram (private communication): an unsmoothed azimuthal sorting of counts in an annulus around the central source between $200''$

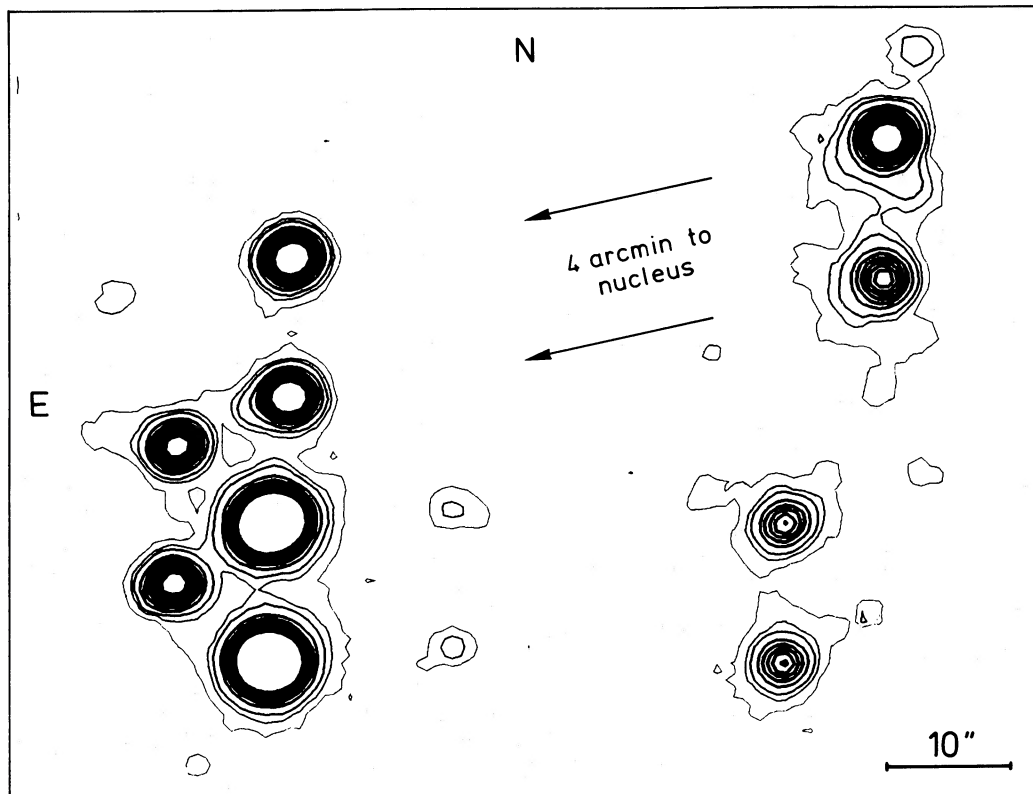


FIG. 1.—Part of the EFOSC image (B-filter) taken through a Savart plate of the western hot spot of Pictor A. Image separation due to the Savart plate is $10''.8$ in approximately north-south direction (N up and E to the left). The high linear polarization of the bright source in the NW corner stands out clearly in comparison to (unpolarized) field objects. It is identified with the western radio hot spot.

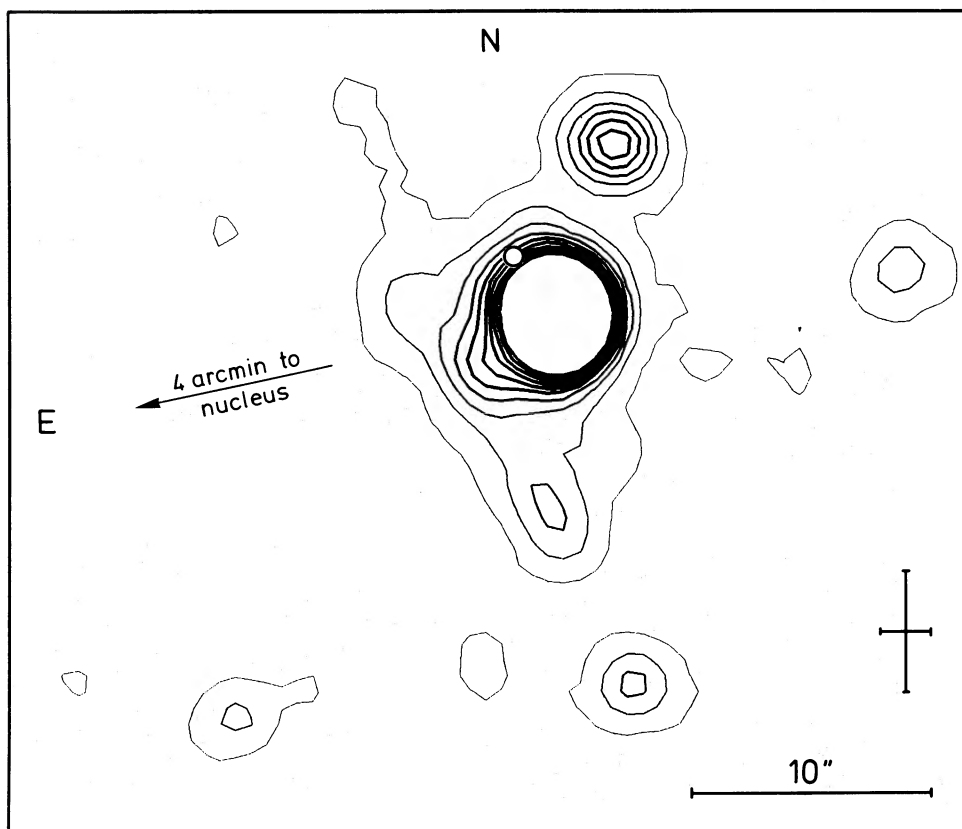


FIG. 2.—Optical counterpart of the western radio hot spot of Pictor A in blue light (2×15 minute EFOSC; N up and E to the left). The unresolved primary maximum is located at $\alpha(1950) = 5^{\text{h}}18^{\text{m}}0^{\text{s}}.09$ and $\delta(1950) = -45^{\circ}48'53''.9$. The VLA position is also indicated by the open circle (O), and the error bar at lower right represents $\pm 1/10$ of the VLA beam size. Note the filaments crossing the hot spot area and the secondary brightness maximum toward the central source.

and $400''$ results in two bins at P.A. 270° and P.A. 300° with 27 and 28 counts compared to a background of 17 counts in other bins. Subtraction of a model point source for the nucleus results in an excess at position $\alpha(1950) = 5^{\text{h}}18^{\text{m}}5^{\text{s}}$, $\delta(1950) = -45^{\circ}48'50''$; that is, $\sim 50''$ to the east of and in good agreement with the optical hot spot position.

IV. DISCUSSION

Given the high linear polarization, its continuous spectrum and the positional coincidence with the VLA position, we regard the source described above as the optical (and possible X-ray) counterpart of the radio hot spot in Pictor A (west).³

Although available observations are far from complete, a few conclusions can already be drawn from the findings reported above. If we assume that the optical polarization is aligned with the intrinsic radio polarization position angle (Haves 1975), an optical polarization of higher than 55% would result. Should this extreme value be confirmed by further optical polarization measurements, we would have a direct clue to the three-dimensional orientation and thus geometry of the object producing the hot spot. A Laing sheet (Laing 1980), for example, has to be viewed almost edge-on to produce these polarization properties. Any diluting radiation as in the case of the 3C 273 jet (RM) could be excluded.

³ We cannot, of course, completely rule out that the object is a BL Lacertae object projected onto the radio lobe. However, the filamentary structure and intrinsic radio polarization angle of 100° (Haves 1985), i.e., along the source axis, argue against that possibility (see Begelman, Blandford, and Rees 1984, p. 274).

Further support for a synchrotron origin is provided by the continuum shape of the radio and optical radiation. Consistent flux values could be determined in the range $14.64 < \log \nu < 14.82$ from the two “blue” spectra. They resulted in a spectral index of -1.2 ± 0.1 , just in accordance with the value for the radio-to-optical index of -0.89 . The observed X-ray flux, which is admittedly rather uncertain because of the low signal-to-noise ratio and poor resolution of the *Einstein* IPC observations, lies only slightly below an extrapolation of this power law to X-ray frequencies (Fig. 5). If confirmed, the X-ray emission would be the most exciting aspect of the hot spot: an inverse Compton origin of the emission seems highly unlikely unless the magnetic field strength in the hot spot is far below its equipartition value of 530 nT or a large fraction of the radio-optical radiation is generated in an extremely compact source ($d < 1$ mpc). On the other hand, thermal bremsstrahlung of a 10^8 K plasma confined to the (unresolved) hot spot would require an uncomfortable high particle density of 1 cm^{-3} . Thus we regard a pure synchrotron origin as the most plausible explanation of the entire radio to X-ray spectrum of the hot spot.⁴ Even with optimistically high estimates of the equipartition magnetic field, the Lorentz factors of the X-ray emitting electrons would then have to exceed 5×10^6 , i.e., we are dealing with TeV particles! Thus the western hot spot of Pictor A differs drastically from the

⁴ A straight power law of index -0.89 joining the radio and the optical data would have to steepen only slightly in order to meet the X-ray point (optical to X-ray spectral index is -1.01 ; see Fig. 5).

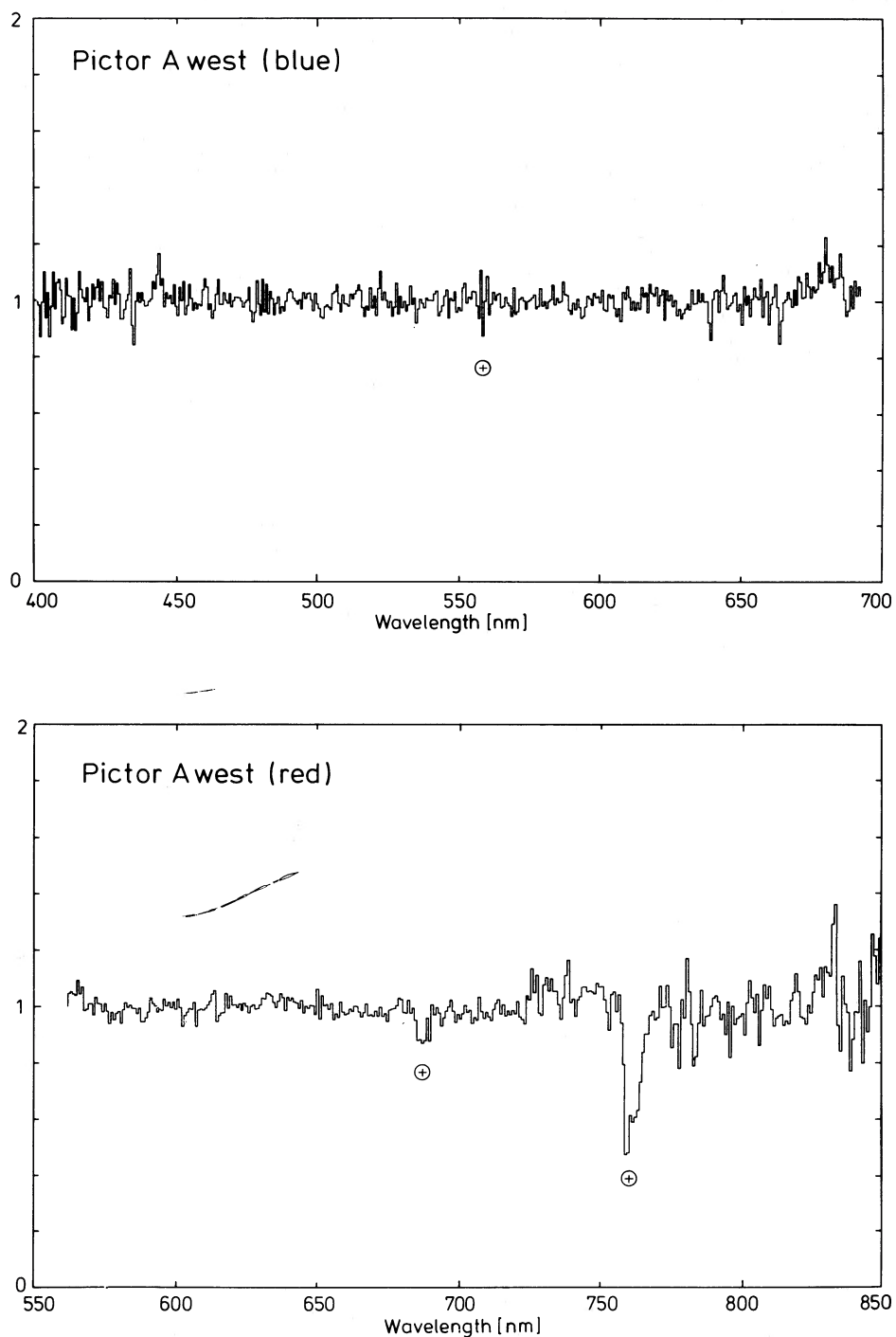


FIG. 3.—Sky-subtracted and normalized EFOSC spectra of the optical counterpart of Pictor A (west) at 0.8 nm resolution. Atmospheric features are indicated by a plus sign within a circle (\oplus). Shortward of 400 nm and longward of 800 nm the count rate was very low. No significant features are seen. *Top*: blue part. *Bottom*: red part.

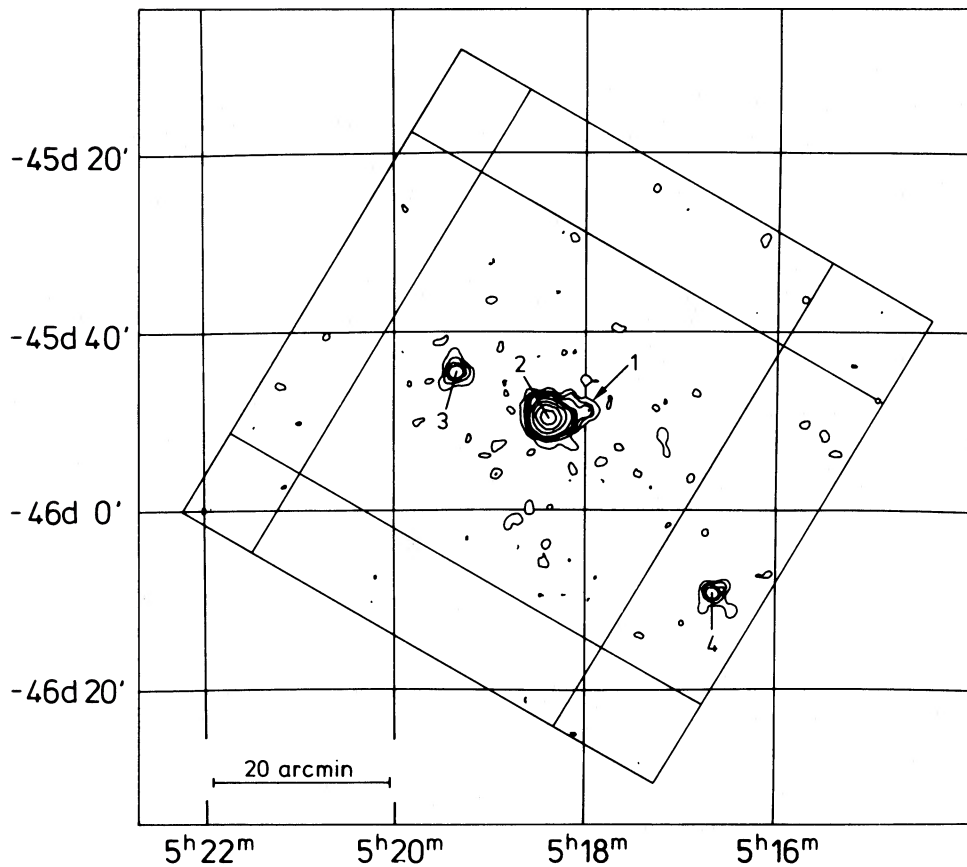


FIG. 4.—*Einstein Observatory* IPC frame of the field of Pictor A (0.2–4 keV). The extension (1) from the central source (2) at P.A. 280° is tentatively identified with the western radio hot spot. Its brightness was estimated to be slightly less than the two serendipitous sources (3, 4). They have a flux at 5×10^{17} Hz of (90 ± 20) nJy and (130 ± 30) nJy, respectively.

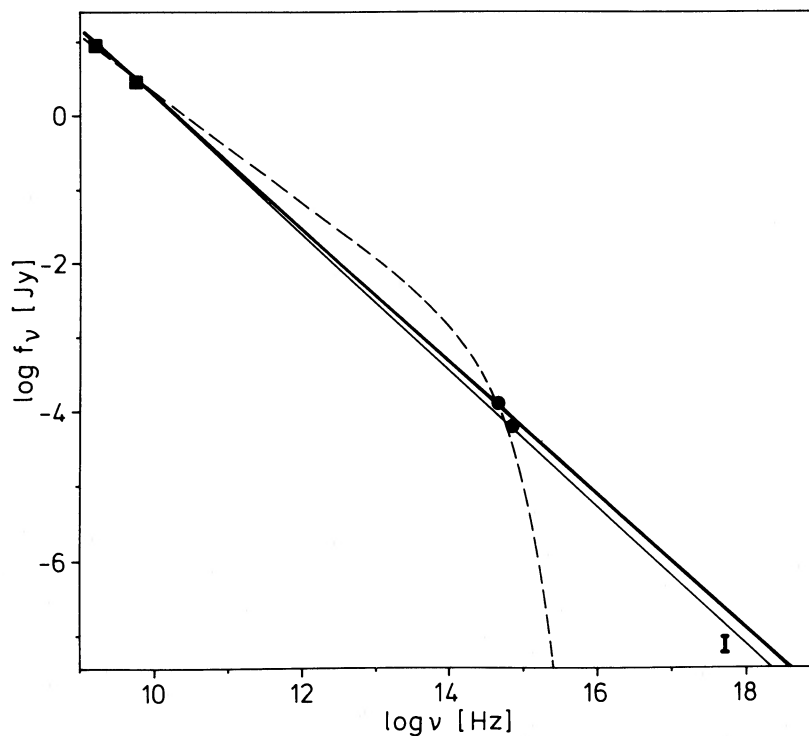


FIG. 5.—Overall spectrum of the western hot spot in Pictor A from VLA data (■; Prestage 1985), optical data (●; this paper) and X-ray data (I; *Einstein Observatory*). The error of the optical data is represented by the symbol size. For the X-ray data an upper limit to the flux equal to the fainter serendipitous source and a lower limit half as large are assumed. The two power-law spectra are derived from all data points (*thin line*) and for radio-to-optical data only (*heavy line*). The cutoff spectrum with index -0.75 , the steepest tabulated by Pacholczyk (1977), and with a critical frequency identical to 3C 33 (south) (MR) is given for comparison (*dashed line*).

other hot spots we studied so far at optical wavelength (3C 273 [see RM]; and 3C 33 [(south); see MR]). For these we found radio-to-optical synchrotron spectra which abruptly steepen above critical frequencies of $\sim 2 \times 10^{14}$ Hz, indicative of a high energy cutoff in the underlying particle distribution (Pacholczyk 1970, 1977).

In summary, Pictor A reveals extraordinary properties. Because of its proximity ($1''$ corresponding to 650 pc, $H_0 = 75$ km s $^{-1}$ Mpc $^{-1}$) and high optical brightness, it opens up

unique possibilities to study the physics in radio hot spots with great detail.

We are very much in debt to Daniel Hofstadt and his staff in La Silla for their excellent support of our observing run. We thank Fred Seward and Sharene Aram from CfA, who kindly supplied the *Einstein* data so rapidly and also for analyzing for us the significance of the X-ray counterpart. Discussions with R. Schlickeiser are also kindly acknowledged.

REFERENCES

- Begelman, M. C., Blandford, R. D., and Rees, M. J. 1984, *Rev. Mod. Phys.*, **56**, 255.
 Buzzoni, B., et al. 1984, *ESO Messenger*, **38**, 9.
 Christiansen, W. N., Frater, R. H., Watkinson, A., O'Sullivan, J. D., and Lockhardt, I. A. 1977, *M.N.R.A.S.*, **181**, 183.
 Crane, P., Tyson, J. A., and Saslaw, W. C. 1983, *Ap. J.*, **265**, 681.
 Haves, P. 1975, *M.N.R.A.S.*, **173**, 553.
 Jenkins, C. J., Pooley, G. G., and Riley, J. M. 1977, *Mem. R.A.S.*, **84**, 61.
 Laing, R. A. 1980, *M.N.R.A.S.*, **193**, 439.
 ———. 1984, in *Proc. NRAO Workshop 9, Physics of Energy Transport in Extragalactic Radio Sources*, ed. A. H. Bridle and J. A. Eilek (Greenbank: NRAO), p. 276.
 Meisenheimer, K., and Heavens, A. F. 1986, *Nature*, **323**, 419.
 Meisenheimer, K., and Röser, H.-J. 1986, *Nature*, **319**, 459 (MR).
 Pacholczyk, A. G. 1970, *Radio Astrophysics* (San Francisco: Freeman).
 ———. 1977, *Radio Galaxies* (Oxford: Pergamon).
 Prestage, R. M. 1985, Ph.D. thesis, University of Edinburgh.
 Röser, H.-J. 1981, *Astr. Ap.*, **103**, 374.
 Röser, H.-J., and Meisenheimer, K. 1986, *Astr. Ap.*, **154**, 15 (RM).
 Schilizzi, R. T., and McAdam, W. B. 1975, *Mem. R.A.S.*, **79**, 1.
 Schwarz, U. J., Whiteoak, J. D., and Cole, D. J. 1974, *Australian J. Phys.*, **27**, 563.

KLAUS MEISENHEIMER: Royal Observatory, Edinburgh EH9 3HJ, Scotland, UK

HERMANN-JOSEF RÖSER: Max-Planck-Institut für Astronomie, Königstuhl, D-6900 Heidelberg 1, West Germany